arXiv:1402.7280v1 [q-bio.MN] 28 Feb 2014

Motif statistics of artificially evolved and biological networks

Burçin Danacı[1], Mehmet Ali Anıl[2] and Ayşe Erzan[1]
[1] *Department of Physics Engineering,Istanbul Technical University, Maslak, Istanbul, Turkey*
[2] *Department of Physics, University of Colorado, Boulder, Colorado, USA*
(Dated: March 3, 2014)

Topological features of gene regulatory networks can be successfully reproduced by a model population evolving under selection for short dynamical attractors. The evolved population of networks exhibit motif statistics, summarized by significance profiles, which closely match those of *E. coli, S. cerevsiae* and *B. subtilis*, in such features as the excess of linear motifs and feed-forward loops, and deficiency of feedback loops. The slow relaxation to stasis is a hallmark of a rugged fitness landscape, with independently evolving populations exploring distinct valleys strongly differing in network properties.

I. INTRODUCTION

Dynamical biological networks, such as gene regulatory networks (GRN) have been the subject of intensive study over more than thirty years [1–8]. It is generally agreed that topology is the main determinant of the dynamical behavior. Milo et al. [9] have introduced the useful concept of network motifs, and shown the predominance of feed-forward loops in biological contexts. The significance profiles of the motif composition of several transcriptional GRNs reveal a marked enhancement of feed-forward loops and an equally marked absence of feed-back loops [10] (also see Klemm and Bornholdt [11].)

The viability or usefulness of biologically meaningful regulatory networks usually require the dynamics to have a point attractor [12, 13], or a small number of multistationary states [2, 14–17]. This is easy to understand e.g., in the context of tissue differentiation, where an embryonic cell is once and for all committed to a particular tissue type, or within the context of periodic behavior such as the diurnal cycle.

In this study, which builds upon and extends previous work [18], we show that simply adopting a fitness function which favors short attractor lengths (point attractors and two-cycles) is sufficient to evolve, via a genetic algorithm [19], populations of regulatory networks with topological properties found in real-life gene regulatory networks. The adjacency matrix of each random graph can be considered as its "genotype." The "phenotype" of the network is the set of its dynamical attractors. The connection between the wiring (the genotype) and the dynamics (the phenotype) is a subtle one, allowing many different types of solutions. By considering many different, independently evolving populations, we are able to observe if interrelations exist between properties such as the mean degree, the motif statistics and the average length and number of attractors.

The significance profiles of the motif frequencies of different populations of evolved networks show a marked resemblance to those found by Milo et al. [10] for real gene regulatory networks. Our results are consistent with earlier findings that the number of feed back loops are suppressed [2, 11] while there is a relatively high frequency of feed-forward loops [9] in biologically relevant regulatory networks.

The evolutionary paths followed by the different populations can be very different from each other, nevertheless yielding the desired characteristic of short attractors. This is an indication of a rugged fitness landscape with divergent valleys (where the mean attractor length is minimized), and is reflected in the slow relaxation of the evolutionary process.

In Section 2 we outline our model. In Section 3 we present our simulation results. Section 4 provides a discussion of our findings.

II. THE MODEL

Our model networks [18] consist of N nodes. Initial populations of random directed networks are generated with an initial connection probability p_0. Each element of the initial adjacency matrix $\mathbf{A}$ independently, assumes values 1 with probability p_0 and 0 with a probability $1 - p_0$ [21]. The directed edges connecting a pair of vertices (i, j) are assigned independently of each other. Counting each directed edge separately, the total number of directed edges is given by $E = \sum_{ij} A_{ij}$. The in- and out-degrees of each node are initially independent and distributed according to a Poisson distribution with the mean p_0N, and $\langle E\rangle_0 = 2p_0N$. On the other hand the total connection probability between any two vertices is $p_0(2 - p_0)$.

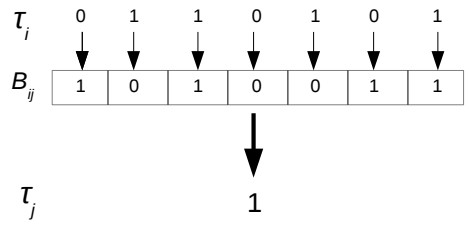

FIG. 1. Inputs τ_i from the neighbors of the jth node and the Boolean key $\mathbf{B}_j$ determine the output τ_j according to Eq.(1).

Variables $\tau_i,\ i = 1 \ldots N$ which can take on the values of 1 or 0, correspond respectively, to an active or a passive state of the node, as in the case of gene regulatory networks. The state of the system is given by the vector $\boldsymbol{\tau}$.

The dynamics can be specified in two equivalent ways. We assigned a random vector, a Boolean "key" $\mathbf{B}_j = (B_{1j}, \ldots, B_{ij}, \ldots, B_{Nj})$ to each jth node, with the entries having the values 0 and 1 with equal probability. All the networks have identical set of keys associated with their nodes. The keys are randomly generated once and for all in the beginning of the simulations, and have the convenient function of labeling the nodes. The nature of the interactions between pairs of nodes are predefined and mutations only affect the topology of the graphs by changing the adjacency matrices. The entries $B_{ij} = 0$ or 1, correspond to an activating or suppressing interaction respectively. (see Fig. 1) The synchronous updating is given by a majority rule,

$$\tau_j(t+1) = \Theta_{\mathrm{H}} \left(\sum_i^N A_{ij} \left[\tau_i(t) \text{ XOR } B_{ij} - \frac{1}{2} \right] \right) \quad . \quad (1)$$

The Heaviside step function is defined as

$$\Theta_{\mathrm{H}}(x) = \begin{cases} 1 & \text{for } x \geq 0 \\ 0 & \text{for } x < 0 \end{cases} . \quad (2)$$

If there are no incoming edges to the node, j, i.e., or $k_j = \sum_i A_{ij} = 0$, then $\tau_j(t+1) \equiv \tau_j$. It is clear that the two states (active/silent) of a node can just as well be represented by Ising spins $s_i = 2\tau_i - 1 = \pm 1$. In this case it is convenient to think of the set of Boolean vectors $\mathbf{B}_j$ as an interaction matrix and to define $\sigma_{ij} = 2B_{ij} - 1 = \pm 1$, with ± 1 corresponding respectively to an activating or suppressing interaction. The input $s_i = \pm 1$ from the ith node to the jth node is then processed using σ_{ij}, and the update rule becomes, for $k_j \neq 0$,

$$s_j(t+1) \equiv 2\Theta_{\mathrm{H}} \left(\sum_i^N A_{ij}\sigma_{ij}s_i(t) \right) - 1 \quad . \quad (3)$$

The model is then equivalent to a finite diluted spin glass. This representation also allows us to make direct contact with the work of Thomas and co-workers [2, 14–16].

The population of networks is evolved using a genetic algorithm [19]. The codes used for the simulations can be accessed from [20]. We have chosen the fitness function to depend on the mean attractor length, a, of the network, averaged over the whole phase space, i.e., all possible initial conditions, so that each attractor is weighted by the size of its basin of attraction. The fitness function $f(a)$ favors average attractor lengths $a \leq 2$. Selected networks are cloned and then mutated by rewiring the edges, while preserving the in- and out-degrees of each node.

The steps of the genetic algorithm are as follows:

1) Generate a population consisting of randomly wired Boolean graphs, with randomly generated Boolean keys as described above.

2) Select the graphs to be cloned according to the fitness function $f(a) = P$ for $a \leq 2$, 0 otherwise. The value of $P = 1/2$ was chosen for rapid convergence.

3) Mutate the clones, by randomly choosing two connected pairs of nodes and switching the terminals of the two directed edges. This preserves the in- and out-degrees of each node.

4) Remove an equal number of randomly chosen individuals.

5) Go back to step 2.

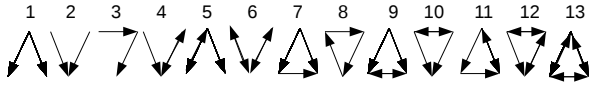

FIG. 2. Three-motifs without self-interactions. Adapted from [10].

In the course of the evolution of the network population, correlations are built up between the edges and the nodes of the networks. Higher order features of network topology, beyond single-site properties such as degree distributions, can be described by the frequencies of common motif structures. Motifs are subgraphs of networks, consisting of three or more connected nodes [9]. Since our networks are small, we considered only 3-motifs and focused our attention on the interactions between the nodes by eliminating self-interactions. This yields a total of 13 motifs shown in Fig. 2. To compare topological features of the resulting graphs to those of randomized graphs, z-scores and significance profiles based on motif frequencies were computed. The z-scores are defined as [9],

$$z_\mu = \frac{\langle N_{\mathrm{evol}}(\mu) \rangle - \langle N_{\mathrm{rand}}(\mu) \rangle}{\sigma[N_{\mathrm{rand}}(\mu)]} \quad (4)$$

where μ is the motif label and $\langle N_{\mathrm{evol}}(\mu) \rangle$ and $\langle N_{\mathrm{rand}}(\mu) \rangle$ are motif frequencies (evolved and randomized, respectively) averaged over 1000 graphs; $\sigma[N_{\mathrm{rand}}(\mu)]$ is the standard deviation. Significance profiles S_μ are obtained by normalizing the z-scores [10],

$$S_\mu = z_\mu \left(\sum_\mu z_\mu^2 \right)^{-1/2} \quad . \quad (5)$$

It should be noted that in Ref. [10] the randomization is carried out while keeping the degree sequence fixed, while we only keep the total number of edges fixed, due to the randomizability problem we encounter with small networks, as explained in the next section.

III. SIMULATIONS

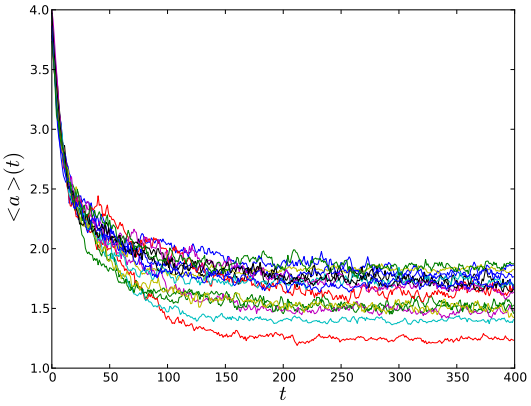

FIG. 3. (Color online) The mean attractor lengths averaged over the whole set, $\langle a \rangle$, v.s. the number of iterations t of the genetic algorithm, for sixteen independent populations with initial expected degree $\langle k \rangle_0 = 3.5$. The initial connection probability of $p_0 = 0.2$ yields qualitatively very similar results (see Supplementary Materials [22]). The rapid decrease is followed by a slow relaxation region before stasis is reached. Thereafter, $\langle a \rangle$ for different populations fluctuates around steady state values. See text.

A. Simulation procedure

Our simulations run for small networks with $N = 7$, for two different sets of populations with initial connection probabilities $p_0 = 0.2$ and $p_0 = 0.5$ (initial mean degrees, $\langle k \rangle_0 = 1.4$ and $\langle k \rangle_0 = 3.5$, respectively). In each case, 16 populations with 1000 networks each were generated. Changes in the mean attractor lengths and in the mean degrees during the simulations are shown in Fig 4 and in Fig 6. Graphs with low mean degrees have lower probabilities of being connected. Therefore, for the populations with $\langle k \rangle_0 = 1.4$, more graphs were generated and only connected ones were kept at each time step. For the populations with $\langle k \rangle_0 = 3.5$, all the generated graphs were kept, since only 74 out of sixteen sets of a thousand graphs each ended up being disconnected.

A randomized control group is used to determine the distinguishing features of the the graphs with short attractor lengths. Randomization was carried out by rewiring the evolved graphs while preserving the total number of edges. Since our networks have relatively few nodes, and since the surviving graphs have typically a smaller density of edges than the initial connection probability p_0, the phase space of possible graphs is very small. This means that rewiring subject to the constraint of preserving the in- and out-degrees very often yields one of the graphs that already belongs to the evolved population, i.e., we have a non-randomizability problem. For this reason, we relaxed this constraint and required

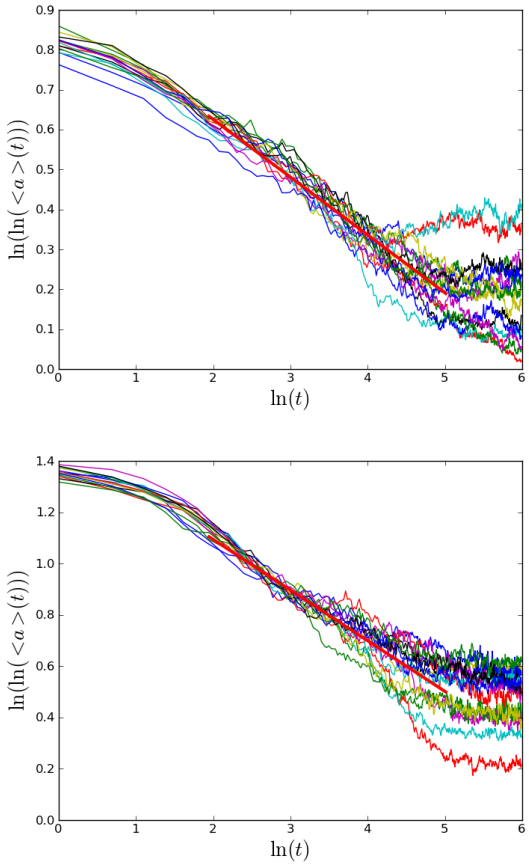

FIG. 4. (Color online) Slow relaxation of the mean attractor lengths. After an initial transient, $\langle a \rangle$ is seen on this on a log-log plot to relax like a power law, $t^{-\gamma}$, for sixteen independent populations with initial $\langle k \rangle_0 = 1.4$ (upper panel) and $\langle k \rangle_0 = 3.5$ (lower panel).The bold red line has been obtained by a simultaneous linear least squares fit over the interval $7 < t < 150$ to the 16 curves, giving $\gamma = 0.15 \pm 0.03$ and $\gamma = 0.20 \pm 0.05$ for the upper and lower panels respectively.

only the total number of edges to be kept constant. Preserving the number of edges constant leads, once more, to disconnected networks after randomization, especially for the populations with $\langle k \rangle_0 = 1.4$. Therefore, more than 60% of the graphs in the randomized counterparts of the sets with initial $\langle k \rangle = 1.4$ ended up being disconnected, whereas this percentage was less than 1% for the randomized counterparts of the sets with $\langle k \rangle_0 = 3.5$.

B. Simulation results

During the simulations, the mean attractor lengths averaged over each independently evolving set of 1000 networks are seen to decrease rapidly for all the sets, and stabilize after around 150-200 time steps (see Fig. 3).

The slow decay of the mean attractor lengths in the course of the evolution can be seen in Fig. 4. We find that we can fit the relaxation curves with a power law

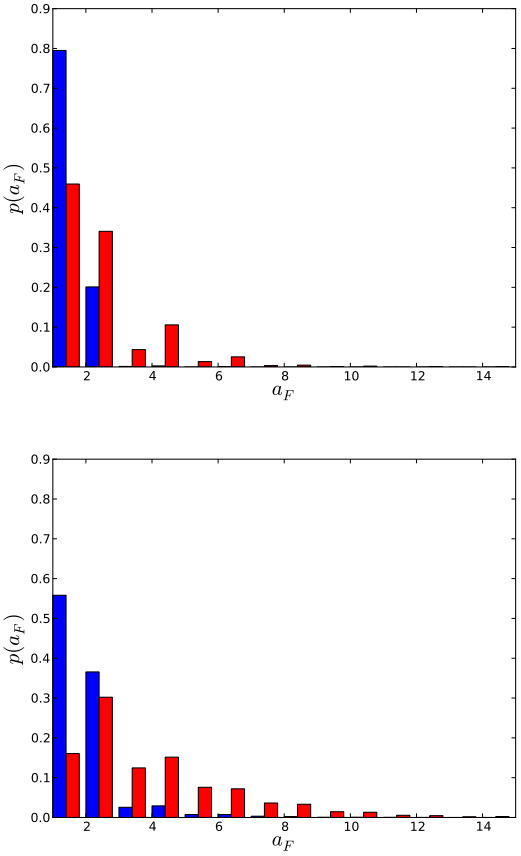

FIG. 5. (Color online) Attractor length at $t = 400$, a_F. Distributions are computed over 16×10^3 graphs and all 2^7 initial states, and are binned into unit intervals. The upper and lower panels are for populations with initial $\langle k\rangle_0 = 1.4$ and $\langle k\rangle_0 = 3.5$. Blue and red bars represent evolved and randomized sets, respectively. In the lower panel, with an initial connection probability $p_0 = 0.5$, the distribution of a_F acquires a longer tail, while the number of attractors decreases (see Fig. 8).

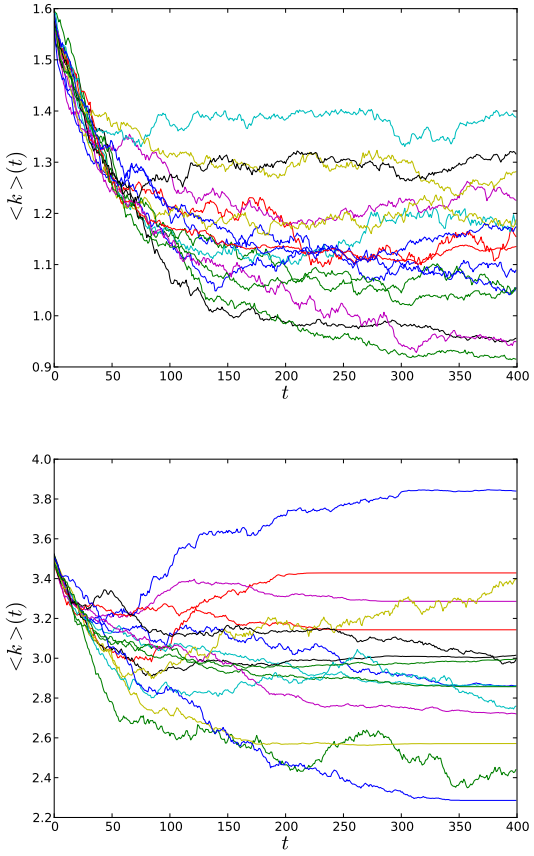

FIG. 6. (Color online) The mean degree $\langle k\rangle(t)$ as a function of the number of iterations of the genetic algorithm, for sixteen independent populations with initial $\langle k\rangle_0 = 1.4$ (upper panel) and $\langle k\rangle_0 = 3.5$ (lower panel).

decay, $\langle a\rangle \sim t^{-\gamma}$, over the interval $7 < t < 150$. The values for the exponents are given in Table 1.

The mean length of the attractors, averaged over all sets and over a time window $300 \leq t \leq 400$, for two different initial connection probabilities are also given in Table 1. The $\langle a\rangle_S$ for each set is within 0.08 of the average attractor length over all the networks within that set taken at an arbitrarily chosen time, $t = 400$, within the steady state regime. (Values for individuals sets can be found in the Supplementary Materials. [22])

As the distributions of attractor lengths at $t = 400$ in Fig. 5 show, about 80% of the networks in the evolved sets with $p_0 = 0.2$, have attractors with mean lengths smaller than 2, whereas the percentage of the networks having attractors with $a < 2$ in the randomized counterparts of the sets with the initial connection probability $p_0 = 0.2$ is about 45%. For the evolved sets with $p_0 = 0.5$ and their randomized counterparts, these percentages are 55% and 15%, respectively.

TABLE I. Parameters for the power law fits to the slow relaxation to stasis, $7 < t < 150$, and the mean attractor lengths $\langle a\rangle_S$, averaged over a hundred steps within the "equilibrium" region, $300 < t < 400$, for two initial connection probabilities. The error bars for γ are calculated from the rms error of the linear fit.

p_0	γ	$\langle a\rangle_S$
0.2	0.15 ± 0.03	1.21 ± 0.12
0.5	0.20 ± 0.05	1.63 ± 0.17

In Fig. 6, we display the mean degree $\langle k\rangle(t)$ averaged over each set, plotted against the number of iterations. In the initial stages of their evolution with the genetic algorithm, the populations tend to undergo large fluctuations in their mean degree before they stabilize in a local minimum of the attractor length. The trajectories shown in Fig. 6 suggest that the fitness landscape is a rugged one, as suggested by the very slow relaxation, with independent populations taking very different evolutionary paths to their respective, relatively well adapted

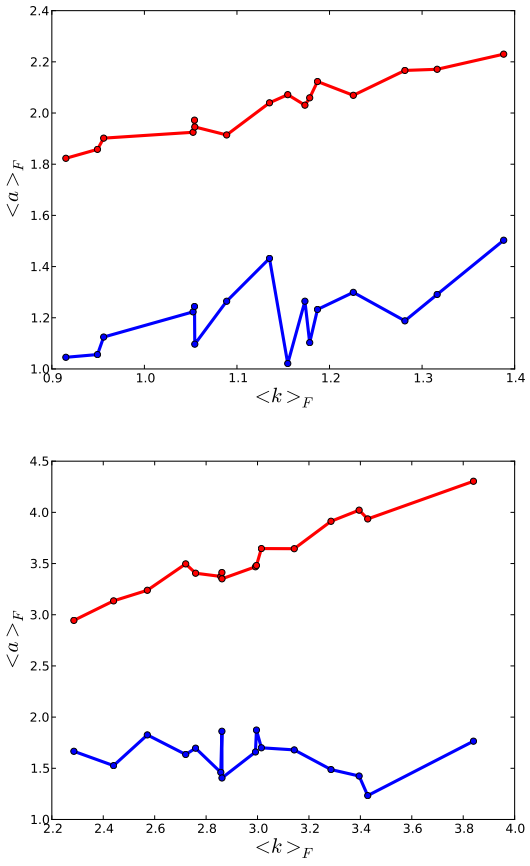

FIG. 7. (Color online) Blue dots indicate population averages of mean attractor lengths $\langle a\rangle_F$ for different populations ranked according to their mean degrees $\langle k\rangle_F$ at $t = 400$. The red dots are the mean attractor lengths for the same population randomized while keeping the number of edges fixed. The upper and lower panels are for populations with initial mean degrees $\langle k\rangle_0 = 1.4$ and $\langle k\rangle_0 = 3.5$ respectively. The lines are a guide to the eye. Note that the horizontal axes in the upper and lower panels have very different scales.

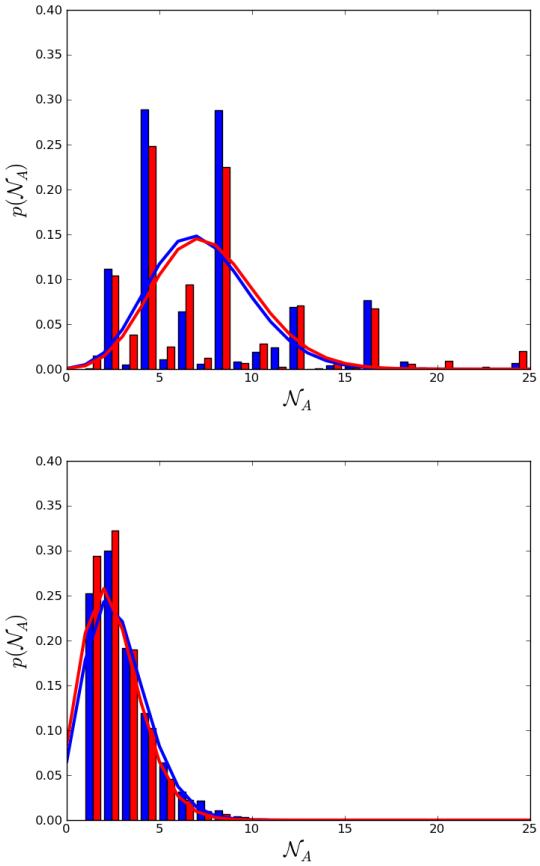

FIG. 8. (Color online) The distributions of number of attractors of populations with initial $\langle k\rangle_0 = 1.4$ (upper panel) and $\langle k\rangle_0 = 3.5$ (lower panel). Blue and red bars represent evolved and randomized sets; the bars are aligned with the integer values and offset by 0.4, respectively. The blue and red curves are Poisson distributions with the same mean as the evolved and the randomized graphs, respectively. We see that, the number of different attractors a model graph has, i.e., multistationarity, is suppressed as the mean degree is increased.

phenotypic distributions. Moreover, the genotypic features (e.g., the mean degree) can vary quite a bit between different well adapted populations.

From Fig. 7 we see that, for the evolved sets, there is no correlation between the mean attractor lengths and the mean degrees. On the other hand, for the randomized sets, there is a clear correlation between the mean degree and the mean attractor length; $\langle a\rangle$ increases with increasing mean degrees $\langle k\rangle$, in general. Aldana et al. have found [5] a similar result for Kauffman networks with random Boolean functions, where a greater density of edges leads to longer attractors.

The averaged distribution of the number of attractors $\mathcal{N}_\mathcal{A}$ of the evolved and randomized graphs is given in Fig. 8. We observe that for $\langle k\rangle = 0.14$, there is a clear dominance of attractors which are transformed to each other under an exchange of 0 and 1 (equivalently ± 1), manifest in the selection of even numbers in the distribution. This is because many nodes do not have any incoming edges, and there are very few with two or more edges incident on them, so there is no frustration. The total number of attractors are much fewer in the $p_0 = 0.5$ networks. The larger initial mean degree ($\langle k\rangle_0 = 3.5$) leads to a larger number of instances where an equal number of 1/0 (± 1) inputs to the nodes lead to a null argument of the Heaviside functions in Eqs.(1,3), which breaks the symmetry in favor of 1 as the outcome, allowing us to observe odd numbers of attractors of a given length.

In Fig. 9 we display our main results for this paper, the significance profiles (SPs) obtained for the 16 independently evolved populations of 1000 model graphs each, for two different initial connection probabilities. These two sets of profiles have all been obtained at the 400th generation of the genetic algorithm, but the profiles show little variation once stasis has been achieved. The similarity between the significance profiles for the empirical

networks and the evolved ones is remarkable, since the only selection pressure placed on the evolving networks was the length of their attractors. A more detailed discussion is provided in the next section.

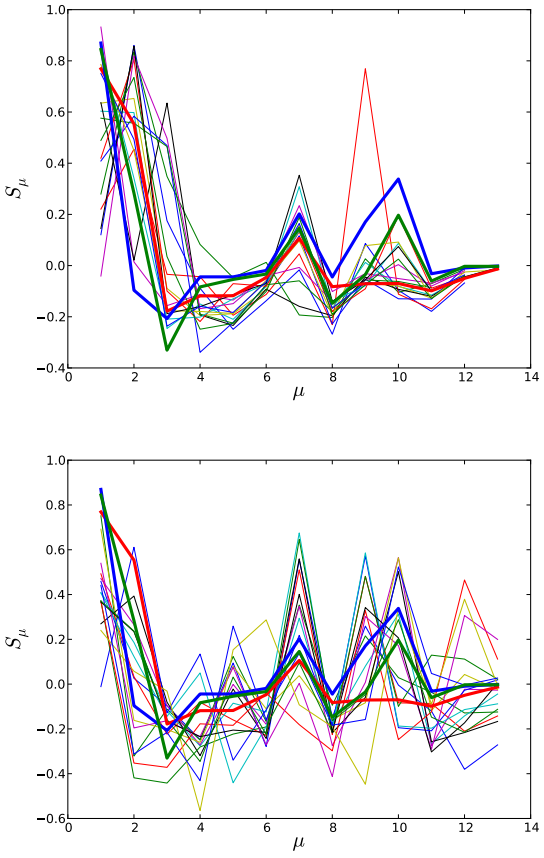

FIG. 9. (Color online) Significance profiles S_μ for populations with initial $\langle k\rangle = 1.4$ (upper panel) and $\langle k\rangle = 3.5$ (lower panel). The horizontal axis runs over the motif labels, μ, while the vertical axis measures the properly normalized, significant deviation of motif frequencies from those encountered in the randomized networks (Eq.5). Thin lines in different colors have been obtained for different model populations, while the bold lines in red, blue and green are the significance profiles of the inner k-cores of the gene regulatory networks of *E. coli, B. subtilis* and *S. cerevisiae* [25], respectively.

IV. DISCUSSION

In this study we have demonstrated that simply constraining the dynamics, to point attractors or at most period-two cycles, is sufficient to artificially evolve populations of model regulatory networks which exhibit topological features found by Milo and co-workers [9, 10] to characterize the gene regulatory networks of a number of organisms.

Our simulations revealed that evolved populations of networks with point attractors or period-two cycles exhibit higher frequencies for certain motifs (Fig. 2) compared to a set of random networks having the same sizes and number of edges (Fig. 9). These are either loopless motifs such as motifs 1, 2, or involve feed-forward loops, such as those numbered 7, 9 and 10 in Fig. 2. On the other hand the motifs 3, 4, 6, 8, 12, and 13 are strongly suppressed in most sets. The motifs 8, 9, 11-13 involve feedback loops which are known [2, 14–16] to give rise to longer attractors for odd number n of negative interactions and multistationarity for even n.

We have also compared our model significance profiles (SPs) with those obtained for real life gene regulatory networks. The empirical networks, which are much larger than our small graphs, are represented here by their innermost k-core [23, 24]. It can be seen from Fig.9 that there are some marked features which are shared by almost all the evolved sets and the core graphs of the transcriptional gene regulatory networks (TGRN) of *E. coli, B. subtilis* and *S. cerevisiae* [25]. The pronounced peaks at motif No. 1,2,7,9,10 and the deep valleys at No. 3,8, as well as the indifferent showing of the motifs No. 4, 11 and 13 are reproduced, even at an exaggerated rate, by more than two thirds of the evolved sets of regulatory networks, for both the initial connection probabilities of 0.2 and 0.5.

The motif statistics taken over the entire regulatory networks [25] are significantly different from what is observed for the core graphs. It should be remarked that the core graphs reveal a lot more structure than the the significance profiles of the whole gene regulatory networks of *E. coli, B. subtilis* and *S. cerevisiae* as reported in [10, 11]. It is interesting that the significance profiles of these core graphs show greater similarity to those of the TGRN of the higher organisms, such as *D. melanogaster* and sea urchin (species unspecified) [10], especially in the region of motifs of greater complexity, 8-13. It can be argued that these subgraphs belong to the most highly connected, computational core of the TGRN and correspond to the genes that play the most crucial role in regulation. (See Supplementary Materials [22] for mean overlaps of the SPs of different sets, as well as their overlaps with the SPs of the TGRNs of *E. coli, B. subtilis* and *S. cerevisiae*, our model species.)

Conditions for multistationarity in the asynchronous dynamics of regulatory networks have been investigated by Thomas and coworkers [2, 14, 15], who have found a rule-of-thumb for feedback loops consisting of three nodes. For asynchronous updates, an even number number of "negative" (repressive) interactions between the nodes leads to the coexistence several stable attractors (depending upon the initial conditions), i.e., multistationarity, whereas an odd number of negative interactions leads to oscillatory behavior. For the synchronous updating rules which we have adopted, the presence of an odd number of repressive interaction within a feedback loop leads to the lengthening of the attractors present. However, our findings are quite independent of the nature (sign) of the interaction, and depend directly on the

topology of the networks, as characterized by their significance profiles. We have performed independent sets of simulations on networks where the Boolean keys (Fig. 1) were set uniformly to 0 or 1 (leading to uniformly repressive or attractive interactions). Although the attractor lengths are uniformly lower for these networks, the significance profiles of the populations evolving under selection for small attractor lengths show the same structures as in Fig.9. (See Supplementary Materials [22]).

Acknowledgments It is a pleasure to acknowledge several useful discussions with Eda Tahir Turan and Neslihan Şengör.

[1] S. A. Kauffman, "'Metabolic stability and epigenesis in randomly constructed genetic nets," J. Theor. Biol. **22** 437 (1969)

[2] R. Thomas, "On the relation between the logical structure of systems and their ability to generate multiple steady states and sustained oscillations," Series in *Synergetics*, vol. 9, (Springer, Berlin 1981) pp. 180193.

[3] S.N. Coppersmith, L. P. Kadanoff, Z. Zhang,"Reversible Boolean networks I: distribution of cycle lengths," Physica D **149** 11 (2001)

[4] S.N. Coppersmith1, L. P. Kadanoff, Z. Zhang, "Reversible Boolean networks II. Phase transitions, oscillations, and local structures," Physica D **157** 54 (2001)

[5] M. Aldana, S. Coppersmith, L.P. Kadanoff "Boolean dynamics with random couplings," in E. Kaplan et al. eds., *Perspectives and Problems in Nonlinear Science* (Springer-Verlag, New York 2003).

[6] B. Drossel, T. Mihailjev, and F. Greil, "Number and length of attractors in a critical Kauffman model with connectivity one," Phys. Rev. Lett. **94**, 088701 (2005)

[7] D. Balcan and A. Erzan, Dynamics of content based networks, V. N. Alexandrov et al. (Eds.): ICCS 2006, Part III, LNCS 3993, pp. 1083-1090 (Springer-Verlag, Berlin 2006).

[8] D. Cheng, H. Qi, IEEE Trans. Automatic Control **55**, 2251 (2010).

[9] R. Milo, S. Shen-Orr, S. Itzkovitz, N. Kashtan, D. Chklovskii, et al. "Network motifs: simple building blocks of complex networks," *Science* **298**, 824-827 (2002).

[10] R. Milo, S. Itzkovitz, N. Kashtan, R. Levitt, S. Shen-Orr, I. Ayzenshtat, M. Sheffer and U. Alon, "Superfamilies of Evolved and Designed Networks," *Science* **303**, 1538-1542 (2004).

[11] K. Klemm and S. Bornholdt, Proc. Natl. Acad. Sci. USA **102**, 18419 (2005)

[12] S. Ciliberti, O.C. Martin, and A. Wagner, "Innovation and robustness in complex gene networks," Proc. Natl. Acad. Sci. USA **104** 13591 (2007)

[13] S. Ciliberti, O.C. Martin, and A. Wagner, PLoS Compt. Biol. **3**, e15 (2007)

[14] R. Thomas, "Laws for the dynamics of regulatory networks," Internat. J. Dev. Biol. **42** 479 (1998).

[15] R. Thomas, M. Kaufman, "Multistationarity, the basis of cell differentiation and memory I." Chaos **11**, 170 (2001).

[16] R. Thomas, M. Kaufman, "Multistationarity, the basis of cell differentiation and memory II," Chaos **11**, 180 (2001).

[17] A. Richarda, J.-P. Cometa, "Necessary conditions for multistationarity in discrete dynamical systems," Discrete Applied Mathematics **155**, 2403 (2007).

[18] M.A. Anıl, "Boolcu ağlarda motif istatistiği için bir model," İTÜ Fizik Mühendisliği Bölümü Bitirme Tezi (A model for motif statistics in Boolean networks, Diploma thesis, Physics Engineering Department, Istanbul Technical University) 2011.

[19] J.H. Holland, *Adaptation in Natural and Artificial Systems* (MIT Press, Cambridge 2001)

[20] Kreveik Module, `https://github.com/kreveik/Kreveik`.

[21] P. Erdös and A. Renyi, Publ. Mat. (Debrecen) **6**, 290ff (1959); P. Erdös and A. Renyi Publ. Mat. Inst . Hung. Acad . Sci. 5, 17 (1960), and P. Erdös and A. Renyi, Bull. Inst . Int. Stat . **38**, 343 (1961); cited in R. Albert and A.-L. Barabasi, "Statistical mechanics of complex networks," Rev. Mod. Phys. **74**, 47 (2002).

[22] Supplementary Materials `https://www.dropbox.com/s/x1n53t5fl5clb3c/Danaci_Evolved_Motif_Statistics_SuppMat.pdf`.

[23] B. Bollobas, *Modern Graph Theory*, (Springer Verlag, New York 1998)

[24] V. Batagelj and M. Zaversnik, "An O(m) Algorithm for Cores Decomposition of Networks," *Advances in Data Analysis and Classification* **5**, 129-145 (2011)

[25] C. Rodríguez-Caso, B. Corominas-Murtraa and R. V. Solé, "On the basic computational structure of gene regulatory networks," *Molecular BioSystems* **5**, 1617-1629 (2009)